PAPER

Nanowire assisted repeatable DEP–SERS detection in microfluidics

IOP Publishing Nanotechnology
Nanotechnology 30 (2019) 475202 (9pp) https://doi.org/10.1088/1361-6528/ab3dc1

Nanowire assisted repeatable DEP–SERS detection in microfluidics

Tingting Ge[1,5], Sheng Yan[2,5], Lingjun Zhang[1], Hong He[1], Li Wang[3], Shunbo Li[3], Yuan Yuan[1,6], Guo Chen[1,6] and Yingzhou Huang[1,4,6]

[1] Chongqing Key Laboratory of Soft Condensed Matter Physics and Smart Materials, College of Physics, Chongqing University, Chongqing, 401331, People's Republic of China
[2] Department of Physics, The Hong Kong University of Science and Technology, Clear Water Bay, Kowloon, Hong Kong, People's Republic of China
[3] Key Laboratory of Optoelectronic Technology and Systems, Ministry of Education, Key Disciplines Laboratory of Novel Micro-Nano Devices and System Technology, School of Optoelectronics Engineering, Chongqing University, Chongqing, People's Republic of China
[4] Chongqing University Industrial Technology Research Institute, Chongqing, 400044, People's Republic of China

E-mail: yuanyuan9215@gmail.com, wezer@cqu.edu.cn and yzhuang@cqu.edu.cn

Received 5 May 2019, revised 30 July 2019
Accepted for publication 22 August 2019
Published 10 September 2019

Abstract

Surface enhanced Raman spectroscopy (SERS) detection in microfluidics is an interesting topic for its high sensitivity, miniaturization and online detection. In this work, a SERS detection in microfluidics with the help of the Ag nanowire aggregating based on dielectrophoresis (DEP) is reported. The Raman intensities of molecule in microfluidics is greatly enhanced in the naturally generated nanogaps of Ag nanowire aggregating modulated by DEP. Firstly, the influence of DEP voltage and time on Ag nanowire aggregating is investigated to figure out the optimal condition for SERS. And then, the SERS intensities of methylene blue and rhodamine6G at various concentration with high reproducibility and uniformity are studied. Furthermore, the experiment data demonstrate this DEP–SERS system could be repeated used for different molecule detections. At last, the SERS of melamine is measured to explore its application on food safety. Our work anticipates this nanowire assisted repeatable DEP–SERS detection in microfluidics with high sensitivity could meet the emerging needs in environmental pollution monitoring, food safety evaluation, and so on.

Supplementary material for this article is available online

Keywords: SERS, Ag nanowire, microfluidics, DEP

(Some figures may appear in colour only in the online journal)

1. Introduction

As an analytical tool to increase the intensity of Raman signals, surface enhanced Raman spectroscopy (SERS) has attracted wide attention among the public [1, 2]. Typically, the noble metal nanostructures (i.e. Au, Ag, Cu) are active SERS materials to provide the enhancement for Raman signals [3, 4]. The SERS phenomenon is primarily a result of localized surface plasmon resonance [5, 6]. LPRS is generated by the excitation of collective electron oscillations within the metallic nanostructure caused by incident light, which leads to a huge enhancement of the optical local-field on the nanoscale. Both theoretical and experimental studies have also demonstrated that electromagnetic hot spots for molecular detection can be formed by introducing plasmonic nanostructures or using SERS substrates inside microfluidic channels in nanoscale gaps between nanostructures [7–9]. With ongoing progress in the development, the application of SERS has been extended to various fields, including

[5] These authors contributed equally to this work.
[6] Authors to whom any correspondence should be addressed.

biomedical detection and environmental safety, due to its ultra-sensitivity, rapid response time, and the ability to generate molecular vibrational fingerprint [10–13]. Among these applications, SERS measurements coupled with microfluidic devices have emerged several useful benefits over conventional macro-environments. For instance, by combining SERS with microfluidic devices, researchers can miniaturize their laboratory setup for SERS quantification, control the movement of particles in the channels, and decrease the assay time and procedures, which provides portability and lower production cost [12, 14–16].

Currently, in the research of SERS in microfluidics, most enhanced substrates consisted of metal nanostructure is directly fabricated in channel. For example, Kang *et al* reported a photoinduced synthesis method for fabricating Ag nanoparticles embedded on the surfaces of ZnO nanowires integrated into the microfluidic system, which promises the detection of glucose solutions with various concentrations [17]. Bai *et al* directly fabricated a 3D microfluidic SERS system based on femtosecond-laser-assisted wet etching for the real-time detection of toxic substances in microchannel [18]. Leem *et al* presented the formation of Ag thin films in a microfluidic channel while the substrate was heated by the polyol method [19]. In addition, other methods, such as photoreduction [16], and optothermal effect [20] have been successfully used to fabricate enhanced substrates. However, it is difficult for the target molecules to reach the enhanced hot spots on the metal surface ($\leqslant$100 nm) of enhanced substrates fabricated in channel, causing some difficulty for SERS detection. Because molecules with low concentrations are flowing in several hundred-microns channel. Therefore, many researchers adopt bonding methods to enable molecules to reach hot spots on the surface of metal structures, which form the simple bioconjugation and simultaneously realize detection of specific molecules [21–23]. As a result, the SERS substrate might be hard to flush (e.g. presence of -HS groups) and ulteriorly bring significant disturbance to the subsequent SERS signal and analysis no matter for the same molecules or other molecules. It is negative for the extending of diverse applications. In other words, these SERS substrates are irreversible after chemical reaction or physical absorbance with analytes, limiting their recyclability. Recently Phan-Quang *et al* included Ag plasmonic colloidosomes (the mixture) into a microfluidic channel for online sequential SERS detection. The method resolves the poor signal reproducibility and stability [24]. However, the sensitivity of the substrate is relatively insufficient. Multiple reports show that the greatest enhancements come from specific hot spots generated by multiparticle coupling aggregation [25–27]. Chrimes *et al* controlled the spacing of Ag nanoparticles in order to promote the aggregation of nanoparticles to produce strong hot spots by dielectrophoresis (DEP). The system demonstrated reusability and high sensitivity of the platform and repeatability of the measurements [3]. Therefore the combination of DEP-microfluidic and SERS offers unique advantages, opening up new opportunities in various research fields.

In this paper, we presented an active microfluidic system that traps Ag nanowires by the DEP forces as they flow in a liquid channel for SERS detection of molecules. We have paid attention to suspended nanowires in microfluidic channel. The rapid aggregation of Ag nanowires can form a 3D network structure between electrodes in the microfluidic channel, which generates the dense nanogaps and further leads the intense SERS high-density hot spots compared with nanoparticles. Due to close plasmon coupling between branches, the 3D network structures of Ag nanowires act as excellent substrates for SERS detection. Moreover, after releasing the external voltage, the nanowires with analytes can be flushed away. The mode of trapping-releasing-trapping enables the SERS detection of various analytes at the same location. More importantly the effects of external DEP voltage and time on nanowires aggregating were investigated to get the optimal capture condition. Appropriate capture conditions enable SERS detection to be completed with a very small amount of sample and achieve comparatively fast detection. The device was repeatedly used to detect various chemical molecules with various concentrations. Ag nanowires trapping process under DEP is reversible, achieving the reusability of the system and repeatability of the measurements. Finally we further presented the detection of melamine in milk based on this platform, demonstrating its application on food safety. These results indicate the microfluidic system prepared by the DEP method can function as SERS substrates for high-sensitive measurements with excellent performance.

2. Methods and experiment

2.1. Material and sample preparation

Silver nitrate ($AgNO_3$, 99.99%), polyvinyl pyrrolidone (PVP, Mw = 58 000, K29-32), rhodamine6G (R6G), methylene blue (MB), melamine ($C_3H_6N_6$, $\geqslant$99.9%), and tween 20 ($C_{58}H_{113}O_{26}$, viscous liquid) were purchased from Shanghai Aladdin biochemical Polytron Technologies Inc. (Shanghai, China). Ethylene glycol (EG) was purchased from Chengdu Kelong Chemical Reagent Factory (Chengdu, China). All chemicals were used directly without further treatment. High-purity deionized water (18.25 MΩ cm) was produced using Aquapro AWL-0502-H (Aquapro International Company LLC., Dover, DE, USA).

The Ag nanowires were chemically synthesized according to a previous synthetic method [28]. The synthetic Ag nanowires colloid was diluted 10 times using the ethanol solution for all subsequent experiments. A solution of ethanol with Tween 20 was ethanol with the addition of 0.1% w/w tween 20. Semi-skimmed milk (Yili, China) was bought from a local supermarket. Ag nanowires solution and probing molecules solution with different concentrations were mixed in a ratio of 1 to 1. In addition, the solvent of melamine aqueous solution is hot water at a temperature of 90 °C.

2.2. Preparation of the DEP microfluidic device

The microfluidic chip with electrodes on the top and bottom glass surfaces was employed and its function for nanowires manipulation was also demonstrated in this study. The

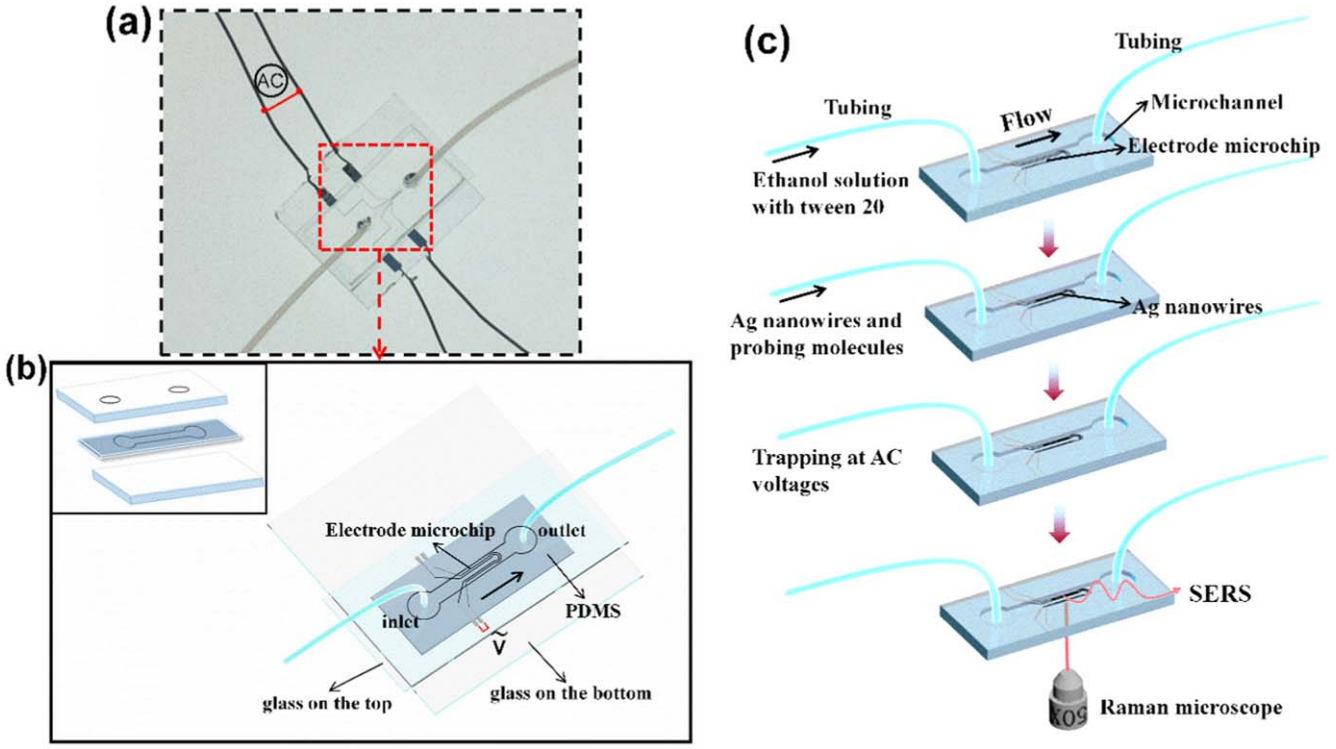

Figure 1. (a) The physical diagram of the DEP microfluidic system. The whole red small boxes represent the magnified area. (b) The completed structure diagram of microfluidic microsystem comprising electrodes. The inset is a explosion view of 3D electrode structure in the microfluidic system (glass-PDMS-glass). (c) The schematic diagram of experimental process.

microfluidic chip was integrated by the microfluidic channel and 3D microelectrodes. The design of the DEP microfluidic device was based on previously published work [29]. The design of the microchip is depicted in figure 1(a). And two holes with the same diameter of 1 mm were drilled on the top glass, which adopted an integrated structure with only one entrance and one exit for more convenience and rapid detection.

2.3. DEP aggregation process of Ag nanowires

The microfluidic channel was washed with the prepared tween 20 ethanol solution prior to use. In doing so, we can prevent Ag nanowires from adsorbing on polydimethylsiloxane (PDMS) for better capture. Next step was to introduce Ag nanowires solution into the microfluidic channel at a low flow rate of 1 μl min^{-1} via a syringe pump (LSP01-2A, Longer Pump). And a function generator (Agilent 33250A) was used to generate a sinusoidal wave with an adjustable frequency and voltage through the wire connections to the microelectrodes. The DEP microfluidic device is applied at a frequency of 20 MHz in the whole experiment. Then the traveling of Ag nanowire was monitored under a microscope and recorded by a CCD camera (Olympus DP73). Finally, the microchannel was again cleaned with the prepared ethanol solution and was pumped at a high flow rate of 100 μl min^{-1} to remove the DEP-captured Ag nanowires rapidly. In this work, the whole experiment was carried out at room temperature and atmospheric pressure.

2.4. Characterization

The DEP–SERS measurements were performed with a home-built setup depicted that was equipped with a 632.8 nm and 10 mW excitation laser in figure S1 (supplementary data is available online at stacks.iop.org/NANO/30/475202/mmedia). A He–Ne laser (Melles Griot) and a spectrometer (iHR550, Horiba, equipped with a charge-coupled device camera) were integrated to an inverted optical microscope (Olympus IX73). All of the Raman spectra were collected under the same ambient conditions. The signals were obtained with one scan every 20 s in all measurements. For acquiring images and videos, an optical microscope coupled to a CCD camera was used. The surface morphology of Ag nanowires trapped by DEP in microfluidic channel was obtained by a field-emission scanning electron microscopy (SEM, TESCAN MIRA 3 FE).

3. Results and discussion

3.1. Preparation DEP–SERS sensor

Figures 1(a) and (b) show the completed structure of microfluidic microsystem comprising 3D electrodes. Furthermore, the explosion view of 3D electrode structure in the microfluidic system is shown in the inset of figure 1(b) (glass-PDMS-glass). As is shown in figure 1(c), the SERS detection of DEP–SERS sensor involves three main steps: (i) washing the microfluidic channel with the prepared ethanol solution, (ii) incorporating the mixture of Ag nanowires and target

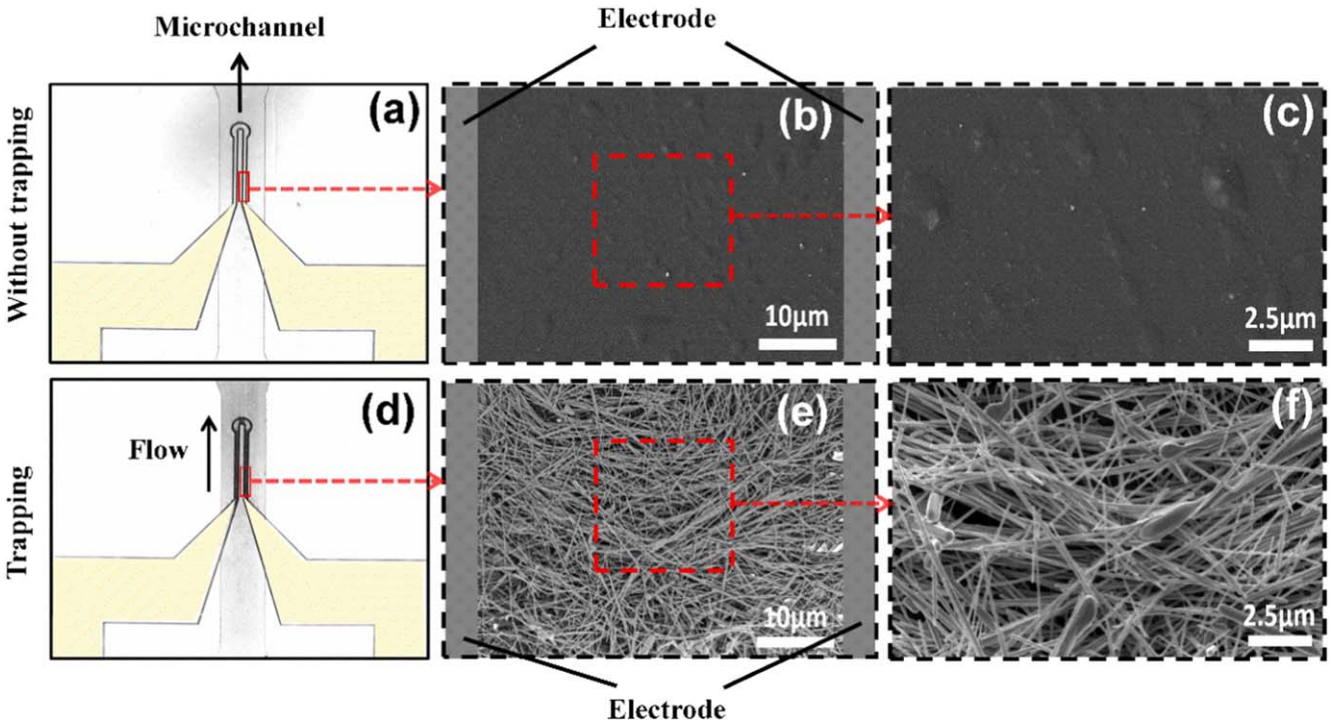

Figure 2. (a) and (d) The optical microscope images of the microeletrodes. (b), (c), (e), and (f) The SEM images of Ag nanowires aggregating between the electrodes with different multiples. The whole red small boxes represent the magnified area.

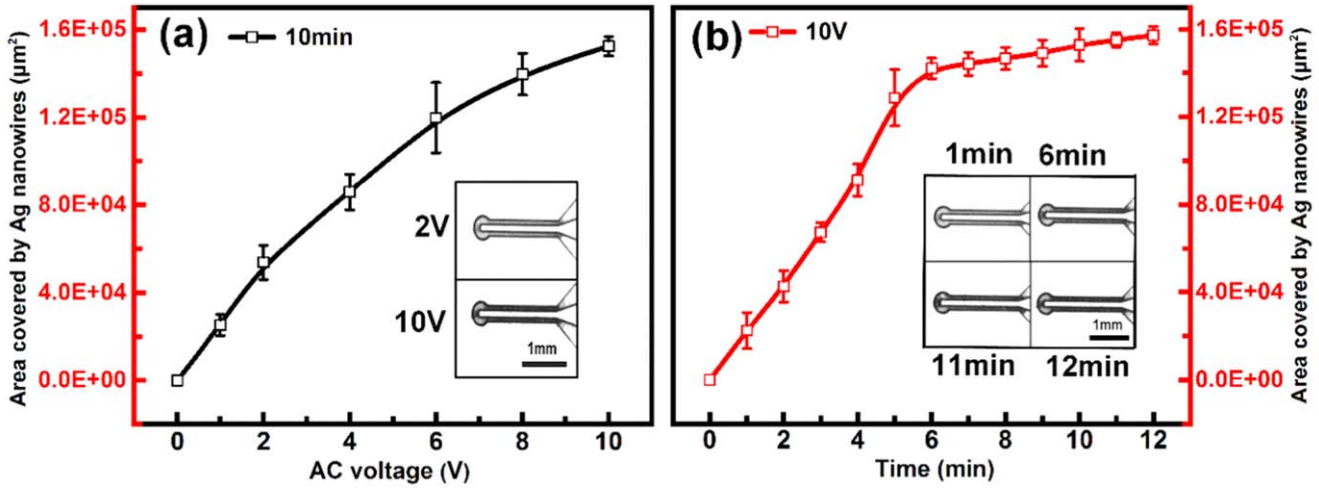

Figure 3. The relation between the AC voltage, the aggregation time and acreages of the black area on electrodes covered by captured Ag nanowires (flow rate: 1 μl min^{-1}; frequency: 20 MHz). (a) The relation between the AC voltage and acreages of the black area on electrodes covered by captured Ag nanowires in 10 min. The inset is a comparison of the acreage of the black area at 2 and 10 V. Error bars are obtained with 3 measurement points. (b) The relation between the aggregation time and acreages of the black area on electrodes covered by captured Ag nanowires at 10 V. The inset is a comparison of the acreage of the black area at 1, 6, 11 and 12 min. Error bars are obtained with 3 measurement points.

molecules with different concentration into the microfluidic channel, (iii) aggregating the mixture at a certain AC voltage and frequency, and then achieving SERS detection. The AC voltage is applied to electrodes to generate the required spatial electric field gradient [7, 29, 30]. In the non-uniform electric field, the Ag nanowires in the vicinity of the electrode can be attracted toward it by DEP force and the Ag nanowires attached to the electrode can generate strong local electric field gradients, thereby attracting other nanowires. A simulation of the electric field distribution in the nanostructure displayed that the strongest gradient of electric field square occurs at the edges of electrodes in figure S2 (supplementary data).

3.2. Trapping of Ag nanowires by DEP

Figure 2 displays the SEM images of Ag nanowires between electrodes under the same conditions when an electric field is

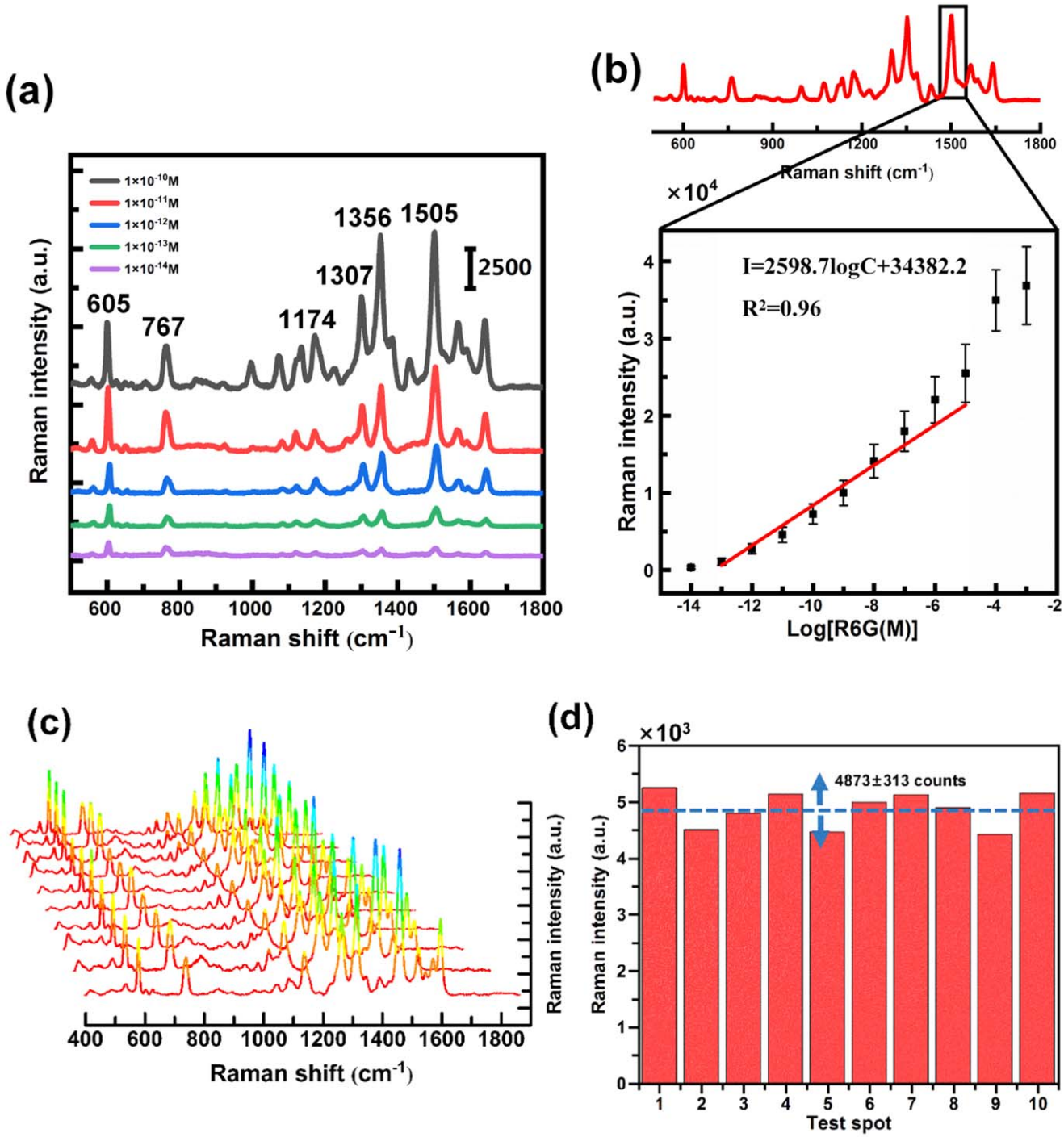

Figure 4. SERS performance of a DEP–SERS system using R6G as a probe molecule. (a) SERS spectra of R6G with concentrations ranging from 10^{-14} to 10^{-10} M on the DEP–SERS system. (b) SERS intensity at 1505 cm^{-1} as a function of R6G concentrations. Each point was obtained from the average of 6 measurements. (c) Reproducibility of the SERS spectra of 10^{-11} M R6G collected at 10 randomly selected spots on the same DEP–SER system. (d) Signal intensity of the 1505 cm^{-1} from 10^{-11} M R6G collected at 10 randomly selected spots on the same DEP–SERS system.

present or absent. When the AC voltage is applied to electrodes, Ag nanowires would concentrate between the microelectrodes as shown in figures 2(d), (e). It is clear that the aggregated Ag nanowires would generate the dense nanogaps, leading the intense SERS high-density hot spots between the electrodes due to close plasmon coupling between branches of 3D network structures. In addition, Ag nanowires could not be attached to the electrode in the absence of AC voltages, as given in figures 2(a)–(c). By contrast, it was easier to promote the agglomeration of Ag nanowires by DEP, thus promoting the increase of SERS hot spots.

Further, to find the excellent performance and the best conditions for Ag nanowire aggregating, we monitored the DEP captured process when changing the DEP voltage and

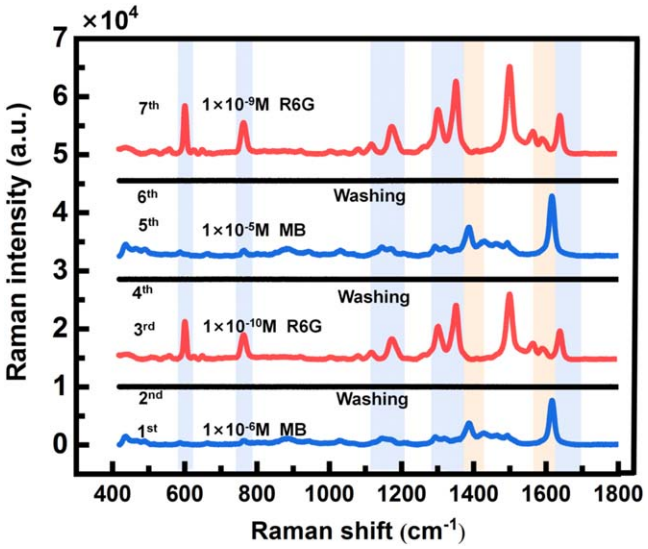

Figure 5. SERS spectra of the R6G and MB with different concentrations obtained alternately on the same position without spectral interference between the analytes.

time, and then calculated the black area on electrodes covered by trapped Ag nanowires using the programming with Matlab. It should be pointed out that the AC voltage and DEP captured time would restrict each other and influence the aggregation of Ag nanowires. To understand more clearly how each factor affects Ag nanowires aggregating, the one variable remains the same and the other one is changed. The 3D microelectrodes are energized by applying with a frequency of 20 MHz, trapping Ag nanowires by DEP at a low flow rate of 1 μl min^{-1}. Figure 3(a) illustrates the black area versus voltage at the aggregation time of 10 min. More remarkably, the area covered by Ag nanowires over the electrodes increases with the increase of the AC voltage. The darker area clearly indicates the superior DEP trapping efficiency of the 3D electrodes with a higher voltage in the inset of figure 3(a). The reason is that the greater the DEP force is generated with the increase of AC voltages. Due to the limitation of AC power supply voltage range, the maximum voltage of this work is 10 V_{p-p}. Then, if the AC power is turned off during the capture process, Ag nanowires aggregating on the electrodes will slowly and automatically disperse and flow out of the microchannel instead of attaching to the electrodes. The entire process containing capturing, dispersing and cleaning is shown in video S1 (supplementary data). It greatly turns out that our DEP microfluidic system is recyclable and reusable, because of the reversibile process of Ag nanowires aggregation process under DEP, which demonstrates high superiority.

Figure 3(b) shows that the area covered by Ag nanowires climbs up as the DEP captured time increases at the same 10 V. After 6 min, the area covered by Ag nanowires increases more and more slowly. To further investigate this matter, we investigated the variations of the depth of the black area in 1, 6, 11 and 12 min, respectively in the inset of figure 3(b). We find the trapped Ag nanowires tends to saturate on the device after 6 min. We chose a capture time of 6 min, because the nanowires increased fastest in the first 6 min, which has created high-density hotspots for SERS detection. And it also shortened the detection time and reduce the number of aqueous samples used in the whole experiment. Compared the curves in figures 3(a) and (b), it could be concluded that the effect of DEP voltage and time on Ag nanowires aggregating has the similar trend at the same flow rate and frequency. The optimal conditions for Ag nanowires aggregating and the SERS detection are at the voltage of 10 V_{p-p} and capture time of 6 min. In this experiment, all measurements were carried under the same concentration of Ag nanowires and under the same equipment.

3.3. SERS performance of the on-chip self-assembly nanowires

Here, using DEP captured Ag nanowires as an enhanced substrate, we evaluated the performance of our DEP–SERS system for the molecular sensing by measuring the SERS responses of R6G on the surface. Notably, to improve the diffusion process of mixing Ag nanowires and analyte molecules, the off-chip mixture was implemented using vortex for 30 s. An AC potential of 10 V_{p-p} (peak-to-peak voltage) at 20 MHz was applied to the electrode leads. And the solutions were pumped at a flow rate of 1 μl min^{-1}. The capture condition of 10 V and 6 min allow us to gain SERS spectrums with a tiny volume of liquid sample. So the SERS spectra of R6G molecules were shown in figure 4(a). All SERS spectrums obtained from the mixture of Ag nanowires and R6G ranging from 10^{-14} to 10^{-10} M, exhibit characteristic vibration performance at 605, 767, 1174, 1307, 1356 and 1505 cm^{-1}. Meanwhile, as the concentration of R6G molecules decreases, the Raman signals become weaker and weaker. The strongest SERS band at 1505 cm^{-1} is selected for comparison of R6G at different concentrations. At first, at a high R6G concentration of 10^{-10} M, a SERS intensity of 7572 $\pm$ 1289 counts is obtained. As R6G molecules solutions are gradually diluted, the SERS intensities reduce and ultimately reaching 329 $\pm$ 169 counts at a R6G concentration of 10^{-14} M. Therefore, the detection limit of our DEP–SERS system is determined to be 10^{-14} M of R6G. The reason for such high sensitivity detection is that R6G molecules placed in the enhanced region of nanogap SERS hot spots and Ag nanowires with R6G molecules are captured between electrodes by DEP. Under the same condition, SERS signals of the pure substrate are not obtained at different time, indicating that the surfactant on the nanowire does not affect the SERS performance of our DEP–SERS system (see figure S3 in supplementary data).

Furthermore, quantitative comparison of the SERS intensities of R6G concentrations shows that a linear SERS response is obtained within the range 10^{-5}–10^{-13} M at the peak of 1505 cm^{-1}, as shown in figure 4(b). The linear relation at 1505 cm^{-1} can be expressed quantitatively as $I = 2598.7\log C + 34382.2$, where C is the R6G concentration expressed in molar concentration and I is the SERS intensity level. And R is the correlation coefficient of linear regression, and R square is equal to 0.96, indicating that this

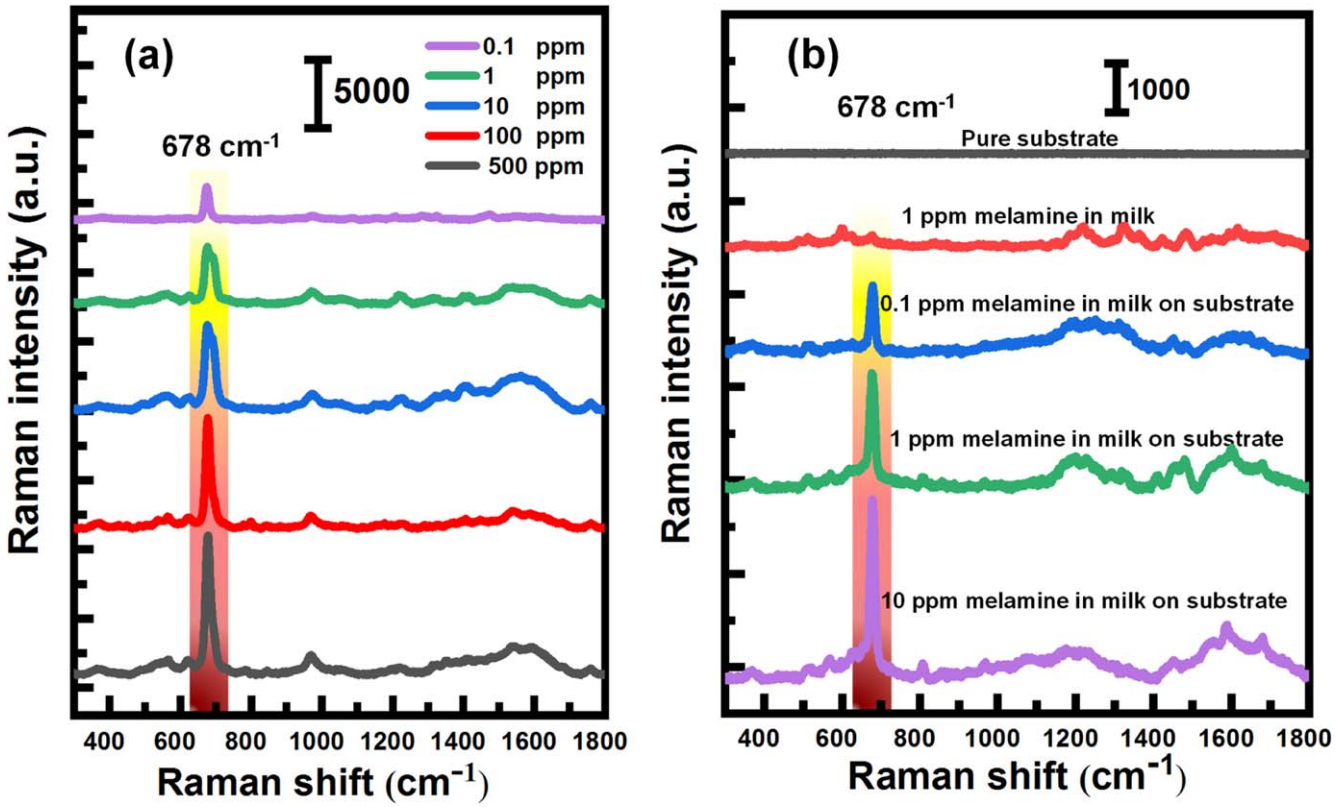

Figure 6. (a) SERS spectra of melamine aqueous solution with concentration ranging from 500 to 0.1 ppm in the DEP–SERS system. (b) SERS spectra of melamine with different concentrations in milk on the DEP–SERS substrate, Raman spectrum of pure 1 ppm melamine in milk and the pure substrate.

curve has a high degree of linear fitting. This result is consistent with the above detection limit studies on a homogeneous SERS substrate, emphasizing the applicability of our DEP device for quantitative detection of analyte molecules. Figure 4(c) shows that with the exception of high sensitivity, the DEP–SERS system provides good spatial uniformity and repeatable SERS signals at a low concentration of 10^{-11} M R6G. Meanwhile, as shown in figure 4(d), a relative standard deviation of the signal changes is less than 6.4% in 10 time measurements at 1505 cm^{-1}, which indicates that the SERS signals enhanced by the DEP–SERS substrate demonstrate excellent reproducibility. The stability of our DEP–SERS system for detect the organic molecules is shown in figure S4 (supplementary data).

3.4. Recyclability of the DEP–SERS system

The recyclability of the DEP device was explored by detecting different kinds of probe molecules alternately. MB and R6G solution with the different concentrations were used as the probe molecules, with entirely different SERS major peaks that could be easily distinguished, as shown in figure 5. Firstly, 10^{-6} M MB solution was injected into the substrate in the microfluidic channels to detect SERS signals (line 1). After washing by the prepared ethanol solution at a high flow rate of 100 μl min^{-1} for 10 min, a featureless SERS spectrum was observed at the second measurement. Then for the third SERS detection on the same position, 10^{-10} M R6G solution was similarly introduced into the microfluidic channel under all the same conditions, the SERS spectrum of which was presented as line 3 in figure 5. This cycle was repeated several times without great changes and shifts of Raman peaks of both MB and R6G and without spectral interference, illustrating the outstanding recyclability of the DEP microfluidic system. Moreover, the recyclability and reusability character greatly promote the utilization and lowers the manufacture cost of the DEP device.

3.5. SERS detection of real samples on the DEP–SERS substrate

To prove the utilization of the DEP–SERS system in practical applications, SERS detection of real samples was taken place on the DEP system using melamine as the target molecules. Melamine was normally adding to the milk formula to artificially inflate the protein content. However, the excessive melamine in milk poses a serious threat to human health, especially for children. Melamine is difficult to metabolize, resulting in varying degrees of renal failure, severe or even death in animals or humans [31, 32]. In fact, the State Food Quality Supervision and Inspection Center of China stipulates that the amount of melamine used in infant formula foods must not exceed 1 ppm, or 2.5 ppm in other foods [33]. Figure 6(a) displays that melamine aqueous solutions with different concentrations were prepared for a serial SERS detection on the DEP–SERS system. The characteristic peak

of melamine at 678 cm^{-1} clearly shows the limit concentration of detection is 0.1 ppm, which is much lower than national standard (2.5 ppm). Further, by directly adding corresponding quantitative melamine into milk to form various gradients melamine solutions, the detection of melamine in real sample was explored. In figure 6(b), the SERS spectrums of melamine in milk with various concentrations on the prepared substrate were compared with the pure substrate and melamine in milk without the substrate. The characteristic peaks of melamine in milk at 678 cm^{-1} are in sharp contrast when the substrate is present or absent, verifying the superiority of the DEP–SERS substrate on food safety application. In the absence of melamine on the pure substrate, SERS spectrum is not obtained in the Raman window, which further confirms that PDMS does not significantly interfere with the high sensitivity application of our DEP–SERS system. Then, the detection limit is as low as 0.1 ppm under the experimental conditions, being far lower than national standard (1 ppm). The presented microfluidic plasmonic sensor provides a powerful analytical tool for detection of melamine in milk.

4. Conclusions

In summary, this work demonstrated a DEP–SERS microfluidic system with the help of Ag nanowires aggregating based on DEP for detection. The optimal condition for SERS detections is obtained by investigating the influence of DEP voltage and time on Ag nanowires aggregating. The SEM images also reveal that Ag nanowires are actively manipulated by the electric field to generate naturally the high-density nanogaps for SERS detection. This device can be used for the analysis of R6G and MB SERS intensities with high reproducibility and uniformity. The detection limit of the DEP–SERS microfluidic system is determined to be 10^{-14} M of R6G. In addition, this microfluidic system can allow the reproducible detection and accurate quantification of analytes with different concentrations. The advantage of substrates prepared in this method is reproducibly dense distribution of hotspots on the surface, increasing the possibility that an target analyte will experience the largest enhancement. Moreover, the nanowires aggregating process under DEP is reversible, allowing the device to be reused for different applications. With all capabilities of the DEP–SERS substrate, we anticipate that it could be developed to meet the emerging needs in environmental pollution monitoring, food safety evaluation, and so on.

Acknowledgments

This work was supported by the National Natural Science Foundation of China (11974067), Fundamental Research Funds for the Central Universities (2019CDYGYB017), Natural Science Foundation Project of CQ CSTC (cstc2019jcyj-msxmX0145), Science and Technology Research Program of Chongqing Municipal Education Commission (KJQN201800101), Key Technology Innovation Project in Key Industry of Chongqing (cstc2017zdcy-zdyf0338) and Sharing Fund of Chongqing University's Large-scale Equipment. Dr Sheng Yan is the recipient of the 2018 Endeavour Research Fellowship funded by the Australian Department of Education and Training.

ORCID iDs

Yingzhou Huang https://orcid.org/0000-0003-1458-4054

References

[1] Feng L J, Fan H Y, Yong D, Lin Y Z, Bo L S, Shun Z X, Ru F F, Wei Z, You Z Z and De Yin W 2010 Shell-isolated nanoparticle-enhanced Raman spectroscopy *Nature* **464** 392–5
[2] Zhang H, Liu M, Zhou F, Liu D, Liu G, Duan G, Cai W and Li Y 2015 Physical deposition improved SERS stability of morphology controlled periodic micro/nanostructured arrays based on colloidal templates *Small* **11** 844–53
[3] Chrimes A F, Khoshmanesh K, Stoddart P R, Kayani A A, Mitchell A, Daima H, Bansal V and Kalantar-zadeh K 2012 Active control of silver nanoparticles spacing using dielectrophoresis for surface-enhanced Raman scattering *Anal. Chem.* **84** 4029–35
[4] Zhang T, Sun Y, Hang L, Li H, Liu G, Zhang X, Lyu X, Cai W and Li Y 2018 Periodic porous alloyed Au-Ag nanosphere arrays and their highly sensitive SERS performance with good reproducibility and high density of hotspots *ACS Appl. Mater. Interfaces* **10** 9792–801
[5] Shi B, Zhou W, Chen T, Oakes K D and Hu A 2014 Laser-processed nanostructures of metallic substrates for surface-enhanced Raman spectroscopy *Curr. Nanosci.* **10** 486–96
[6] Liu T, Hao J, Huang Y, Xun S, Li H and Fang Y 2016 Heterodimer nanostructures induced energy focusing on metal film *Physics* **120** 7778–84
[7] Almeida G B, Poppi R J and Da S J 2016 Trapping of Au nanoparticles in a microfluidic device using dielectrophoresis for surface enhanced Raman spectroscopy *Analyst* **142** 375–9
[8] Hsing-Ying L, Chen-Han H, Wen-Hsin H, Ling-Hsuan L, Yuan-Chuen L, Chia-Chun C, Shi-Ting W, I-Ting K, Lai-Kwan C and Chiou-Ying Y 2014 On-line SERS detection of single bacterium using novel SERS nanoprobes and a microfluidic dielectrophoresis device *Small* **10** 4700–10
[9] Yamaguchi A, Fukuoka T, Takahashi R, Hara R and Utsumi Y 2016 Dielectrophoresis-enabled surface enhanced Raman scattering on gold-decorated polystyrene microparticle in micro-optofluidic devices for high-sensitive detection *Sensors Actuators* B **230** 94–100
[10] Etchegoin P, Maher R C, Cohen L F, Hartigan H, Brown R J C, Milton M J T and Gallop J C 2003 New limits in ultrasensitive trace detection by surface enhanced Raman scattering (SERS) *Chem. Phys. Lett.* **375** 84–90
[11] Wang B, Zhang L and Zhou X 2014 Synthesis of silver nanocubes as a SERS substrate for the determination of pesticide paraoxon and thiram *Spectrochim. Acta* A **121** 63–9
[12] Yuling W, Sakandar R, Grewal Y S, Spadafora L J, Shiddiky M J A, Cangelosi G A, Sebastian S and Matt T 2014 Duplex microfluidic SERS detection of pathogen antigens with nanoyeast single-chain variable fragments *Anal. Chem.* **86** 9930–8

[13] Zhang H, Zhou F, Liu M, Liu D, Men D, Cai W, Duan G and Li Y 2015 Spherical nanoparticle arrays with tunable nanogaps and their hydrophobicity enhanced rapid SERS detection by localized concentration of droplet evaporation *Adv. Mater. Interfaces* **2** 1500031

[14] Zhou Q and Kim T 2016 Review of microfluidic approaches for surface-enhanced Raman scattering *Sensors Actuators* B **227** 504–14

[15] Chung E, Gao R, Ko J, Choi N, Lim D W, Lee E K, Chang S I and Choo J 2013 Trace analysis of mercury(II) ions using aptamer-modified Au/Ag core–shell nanoparticles and SERS spectroscopy in a microdroplet channel *Lab Chip* **13** 260–6

[16] Xu B B, Ma Z C, Wang L, Zhang R, Niu L G, Yang Z, Zhang Y L, Zheng W H, Zhao B and Xu Y 2011 Localized flexible integration of high-efficiency surface enhanced Raman scattering (SERS) monitors into microfluidic channels *Lab Chip* **11** 3347–51

[17] Kang H W, Leem J and Sung H J 2014 Photoinduced synthesis of Ag nanoparticles on ZnO nanowires for real-time SERS systems *RSC Adv.* **5** 51–7

[18] Bai S, Serien D, Hu A and Sugioka K 2018 3D microfluidic surface-enhanced raman spectroscopy (SERS) chips fabricated by all-femtosecond-laser-processing for real-time sensing of toxic substances *Adv. Funct. Mater.* **28** 1706262

[19] Juyoung L, Hyun Wook K, Seung Hwan K and Hyung Jin S 2014 Controllable Ag nanostructure patterning in a microfluidic channel for real-time SERS systems *Nanoscale* **6** 2895–901

[20] Yuliang X, Shikuan Y, Zhangming M, Peng L, Chenglong Z, Zane C, Po-Hsun H and Tony Jun H 2014 *In situ* fabrication of 3D Ag@ZnO nanostructures for microfluidic surface-enhanced Raman scattering systems *Acs Nano* **8** 12175

[21] Galarreta B C, Tabatabaei M, Lagugne-Labarthet F, Guieu V and Eric P 2013 Microfluidic channel with embedded SERS 2D platform for the aptamer;detection of ochratoxin A *Anal. Bioanalytical Chem.* **405** 1613–21

[22] Yang M, Alvarez-Puebla R, Kim H S, Aldeanueva-Potel P, Liz-Marzan L M and Kotov N A 2010 SERS-active gold lace nanoshells with built-in hotspots *Nano Lett.* **10** 4013–9

[23] Lin H Y, Huang C H, Hsieh W H, Liu L H, Lin Y C, Chu C C, Wang S T, Kuo I T, Chau L K and Yang C Y 2014 On-line SERS detection of single bacterium using novel SERS nanoprobes and a microfluidic dielectrophoresis device *Small* **10** 4700–10

[24] Phan-Quang G C, Wee E H Z, Yang F, Lee H K, Phang I Y, Feng X, Alvarez-Puebla R A and Ling X Y 2017 Online flowing colloidosomes for sequential multi-analyte high-throughput SERS analysis *Angew. Chem., Int. Ed. Engl.* **56** 5565–9

[25] Asiala S M and Schultz Z D 2011 Characterization of hotspots in a highly enhancing SERS substrate *Analyst* **136** 4472–9

[26] Ying F, Nak-Hyun S and Dlott D D 2008 Measurement of the distribution of site enhancements in surface-enhanced Raman scattering *Science* **321** 388–92

[27] Michaels A M and Jiang L J 2000 Ag nanocrystal junctions as the site for surface-enhanced raman scattering of single rhodamine 6G Molecules *J. Phys. Chem.* B **104** 11965–71

[28] Zhipeng L, Shunping Z, Halas N J, Peter N and Hongxing X 2015 Coherent modulation of propagating plasmons in silver-nanowire-based structures *Small* **7** 593–6

[29] Li M, Li S, Wu J, Wen W, Li W and Alici G 2011 A simple and cost-effective method for fabrication of integrated electronic-microfluidic devices using a laser-patterned PDMS layer *Microfluid. Nanofluid.* **12** 751–60

[30] Tang S Y, Zhu J, Sivan V, Gol B, Soffe R, Zhang W, Mitchell A and Khoshmanesh K 2015 Creation of Liquid Metal 3D Microstructures Using Dielectrophoresis *Adv. Funct. Mater.* **25** 4445–52

[31] Katie B, Scott N, Susan K and Allison R 2007 Recall of pet food leaves veterinarians seeking solutions *J. Am. Veterinary Med. Assoc.* **230** 1136–8

[32] Chan E, Griffiths S M and Chan C W 2008 Public-health risks of melamine in milk products *Lancet* **372** 1444–5

[33] Liu B, Lin M and Li H 2010 Potential of SERS for rapid detection of melamine and cyanuric acid extracted from milk *Sens. Instrum. Food Qual. Saf.* **4** 13–9